COMPUTER SIMULATION OF HIGH-CURRENT ION BUNCHES TRANSPORT AND ACCELERATION WITH ADDITIONAL SPACE CHARGE COMPENSATION BY THERMAL ELECTRONS

O.V. Manuilenko, V.I. Karas'*
National Science Center "Kharkov Institute of Physics and Technology", Kharkov, Ukraine
**E-mail: ovm@kipt.kharkov.ua*

The particle in cell simulation results, within the limits of the complete set of the Maxwell-Vlasov equations, of the short (the ion bunch length is much smaller than the cusp length) and long (the ion bunch length is much longer than the cusp length) high-current compensated tubular ion bunches transportation and acceleration in the peaked fence magnetic field are presented. The ion bunch current, at injection in the cusp, is compensated by an accompanying electron bunch. Additional compensation of the ion bunch space charge by means of thermal electrons generated in the drift space has been studied. It is shown that both for short and for long ion bunches, the optimized additional space charge compensation by thermal electrons leads to a reduction of the energy spread of the accelerated ion beam at the output of the cusp.

PACS: 41.75.-i, 52.40.Mj, 52.58.Hm, 52.59.-f, 52.65.Rr

INTRODUCTION

The usage of linear induction accelerators (LIA) for obtaining high-current ion beams (HCIB) with the parameters required for inertial confinement fusion is perspective, as LIA can operate at high pulse frequency, and can accelerate, with efficiency of 30%, high-current beams of virtually any ions, and perform time compression of current pulse in the acceleration process, which eliminates the operations related to the increase of current due to compression rings. The classical vacuum LIAs are discussed in [1]. The final ions energy at the target should be approximately 10 GeV with energy content of 10 MJ and a pulse duration of a few tens of nanoseconds. The usage of collective focusing methods in the LIA allows significantly increase the ion beam current and decrease its energy while maintaining the required energy content of the beam on the target. In such kind of LIA the ion beam space charge is compensated by electrons [2 - 4], and the electron current is suppressed by magnetic insulation of accelerating gaps [5]. The nature of charge and current neutralization of an HCIB by an electron beam in an axisymmetric accelerating gap was investigated in [5 - 8], where the dynamics of electrons and ions in the cusp magnetic fields in the presence of an accelerating field in the single-particle approximation, and the influence of own electric and magnetic fields of electron and ion beams on the magnetic isolation, and their passage through the cusp have been studied. The transport and acceleration of compensated ion beam in the 1 - 6 cusps was investigated in [9 - 13]. It was shown that the ion energy distribution function of the HCIB at the exit of the accelerator improves with increasing energy of the accompanying electron beam, and that the additional injection of electron beams in the cusps decreases HCIB energy spread and reduces its divergence in space. The transport and acceleration of the short, compared to the cusp length, high-current electron and ion bunches (IB) was studied in [14, 15]. It was shown that additional compensation of the accelerated ion bunch space charge by thermal electrons leads to reduction of its energy dispersion and divergence on an exit from the cusp. It was shown also that overcompensation of the ion bunch space charge by thermal electrons leads not only to increase of energy spread and divergence of an ion bunch on an exit from the cusp, but also to deceleration of an ion bunch.

In this paper we study the acceleration and transport of short and long high-current tubular IBs in the picked fence magnetic field with the additional compensation of IB space charge by thermal electrons. It is shown that both for short and for long IBs, the optimized additional space charge compensation by thermal electrons leads to a reduction of the energy spread of the accelerated IB at the output of the cusp.

Fig. 1 shows the simulated structure, the configuration of the external magnetic field [9, 10] and the place of the electron and ion beams injection. The length of the cusp is z_L = 10.24 cm, its radius is r_L = 10.24 cm, [0, z_I] and [z_{II} , z_L] are the drift spaces, z_I = 4.8 cm, z_{II} = 5.44 cm, [z_I , z_{II}] is the accelerating gap.

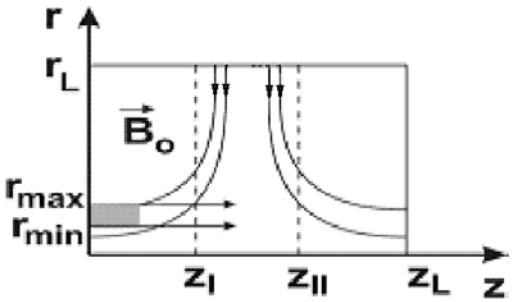

Fig. 1. Configuration of the external magnetic field and regions of electron and ion bunches injection into the computation domain

The minimal and maximal radius of the electron and ion bunches are the same: $r_{\min}$ = 1.32 cm, $r_{\max}$= 1.48 cm. At the injection time $n_{e0}v_{e0} = n_{i0}v_{i0}$, the electron bunch density is n_{e0} = $7.12 \cdot 10^{13}$ cm^{-3}, the electron bunch velocity is v_{e0} = 0.95·c, the initial velocity of the ion bunch (protons) is v_{i0} = 0.285·c, c is the speed of light. The external magnetic field has a cusp configuration [9, 10] with amplitude H_0 = 47 kGs. The IB length is $0.5 \cdot z_I$ (short IB), and $36 \cdot z_I$ (long IB). In computer simulations (see below) in regions $[0, z_i] \times [r_{\min}, r_{\max}]$,

$[z_{II}, z_L]\times[r_{\min}, r_{\max}]$, there were a generation of Maxwellian electrons (ME) with temperature T_e= 1 keV. These electrons are intended to further compensation of the IB space charge. The generation rate is chosen so that at the time of its termination the electron density n_e^{comp} was the specified value. The outer boundaries of the system are perfectly conducting metal walls. Particles that fall into the boundaries are removed from the simulation. Particle in cell simulation scheme is described in detail in [9, 10, 16].

SIMULATION RESULTS

Fig. 2 show the simulation results for the transport of the high-current compensated IB through the cusp with additional compensation of the IB space charge by means of the ME, and without additional compensation. The ion distribution functions (IDFs) depending on energy (IEDF) and transverse coordinate at the exit of the cusp are presented. The IB length is $0.5\cdot z_I$. To generate ME, each of the regions $[0, z_I]\times[r_{\min}, r_{\max}]$ and $[z_{II}, z_L]\times[r_{\min}, r_{\max}]$ is divided into 30 sub-areas $[z_I{}^j, z_I{}^{j+1}]\times[r_{\min}, r_{\max}]$ and $[z_{II}{}^k, z_{II}{}^{k+1}]\times[r_{\min}, r_{\max}]$ of equal length in the longitudinal direction. In each subdomain the generation of ME starts at the moment when the front of the IB crosses its left edge, and ends when the front of the IB crosses its right edge. The generation rate is chosen so that at the time of its termination the ME density $n_e^{comp} = 0.7\ n_{i0}$. In this case $n_{e0} + n_e^{comp} = n_{i0}$. Fig. 2,a – no ME generation, Fig. 2,b – the generation of ME only in the right half of the cusp, Fig. 2,c – the generation of ME only in the left half of the cusp, Fig. 2,d – the generation of ME in the left and right halves of the cusp.

As can be seen from Fig. 2, the IB is well focused in the transverse direction. However, after passing the cusp, IEDFs differ greatly and depends on the location in which the ME are generated. If the space charge of the IB is compensated with ME in the right half of the cusp (see Fig. 2,b), the IEDF is almost monochromatic. The additional compensation of the IB space charge in the left half of the cusp (see Fig. 2,c), or in the left and right semicusps (see Fig. 2,d), leads to a considerable spread in ion energy. The increase in the ion energy spread can be explained by the fact that the compensating ME loaded IB, taking part its kinetic energy. This is clearly seen in the ME energy distribution function on the right edge of the cusp – ME from the left side of the cusp always have an average energy exceeding the initial one. Thus, the optimal is the compensation after the accelerating gap.

Fig. 3 show the simulation results for the acceleration of the high-current compensated IB in the cusp. The accelerating potential is 1 MB. IDFs depending on energy and transverse coordinate at the right cusp boundary are presented. Fig. 3,a – no ME generation, Fig. 3,b – the generation of ME only in the right half of the cusp, Fig. 3,c – the generation of ME only in the left half of the cusp, Fig. 3,d – the generation of ME in the left and right halves of the cusp. The generation rate is chosen so that at the time of its termination the ME density $n_e^{comp} = 0.7\ n_{i0}$.

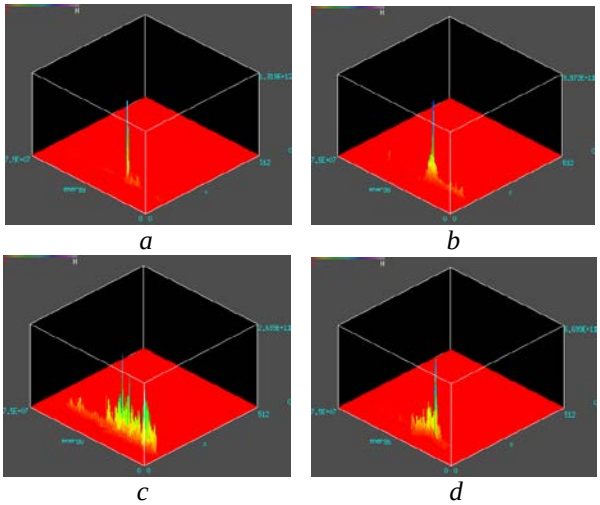

Fig. 2. IDFs vs energy and transverse coordinate at the exit of the cusp: a – the generation of ME is absent; b – ME generated in the right half of the cusp; c – ME generated in the left half of the cusp; d – ME generated in the left and right halves of the cusp. At the time of the termination of the ME generation $n_e^{comp} = 0.7\, n_{i0}$. Accelerating potential is 0 MB

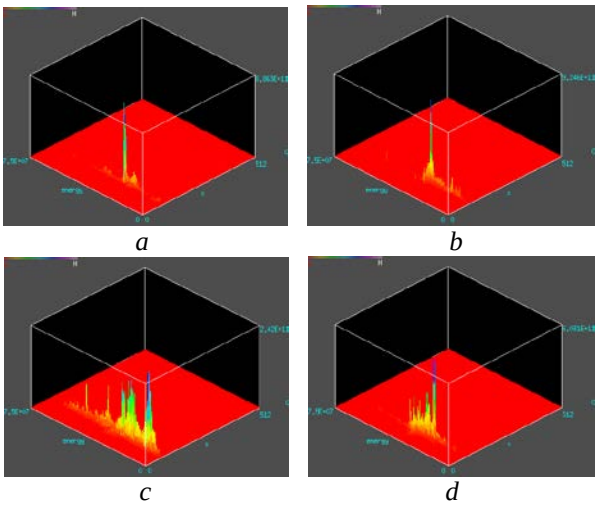

Fig. 3. IDFs vs energy and transverse coordinate at the exit of the cusp: a – the generation of ME is absent; b – ME generated in the right half of the cusp; c – ME generated in the left half of the cusp; d – ME generated in the left and right halves of the cusp. At the time of the termination of the ME generation $n_e^{comp} = 0.7\, n_{i0}$. Accelerating potential is 1 MB

As can be seen from Fig. 3, IBs are well focused in the transverse direction, however, as in the case of transport, after the passage of the cusp, the IEDFs are significantly different depending on the location, where the compensating ME are generated. The IEDF is much more monochromatic, if the space charge compensation of the accelerated IB, using ME, takes place in the right half of the cusp, i.e., after the accelerating gap (see Fig. 3,b), in comparison with the compensation of the accelerated IB in the left half of the cusp (see Fig. 3,c), or in the left and right semicusps (see Fig. 3,d). The increase in the ion energy spread can be explained, as in

the case of transport, by the fact that the compensating ME loaded IB, consuming part its its kinetic energy. This is clearly visible from the ME energy distribution function on the right boundary of the cusp – ME from the left side of the cusp always have an average energy exceeding the initial one. Thus, the optimal space charge compensation of the IB is the compensation after the accelerating gap.

Fig. 4 show the computer simulation results for transport and acceleration of long compensated high-current IB (bunch length $36 \cdot z_I$) without additional IB space charge compensation by thermal electrons. The IDFs depending on energy and transverse coordinate on the right edge of the cusp are presented. Fig. 4,a – the accelerating field is absent, Fig. 4,b – the accelerating potential is 1 MB. The behavior of IEDs on the accelerator output, depending on the accelerating potential, do not differ significantly from the previously studied case of "infinitely long" beam [9 - 13]. Since the accompanying electron beam kinetic energy is enough to overcome the potential in 1 MV for ion acceleration, the electron beam does not load the ion beam. And, therefore, the IDF energy width on the right edge of the cusp, at an accelerating potential of 1 MV, practically does not differ from the IDF energy width in the absence of the accelerating field.

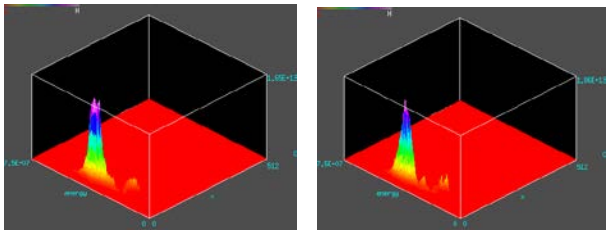

a *b*

Fig. 4. IDFs vs energy and transverse coordinate at the exit of the cusp: a – the accelerating potential is absent; b – the accelerating potential is 1 MB

Fig. 5 show the computer simulation results for the acceleration of long compensated high-current IB (bunch length $36 \cdot z_I$) with additional IB space charge compensation by thermal electrons. The accelerating potential is 1 MB. The ME generation occurs only in the right half of the cusp – in the region $[z_{II}, z_L] \times [r_{\min}, r_{\max}]$ (see Fig. 1). The ME generation starts at a time when the leading edge of the IB cross the left border of the drift gap, and ends when the leading edge of the bunch cross right border of the drift gap. The generation rate is chosen so that at the time of its termination the ME electron density n_e^{comp} is $0.5\, n_{i0}$ (undercompensation) (see Fig. 5,a), $0.7\, n_{i0}$ (see Fig. 5,b), and $1.0\, n_{i0}$ (overcompensation) (see Fig. 5,c).

As can be seen from Fig. 5,a, the additional compensation of the IB space charge by thermal electrons leads to a decrease in ion energy spread at the exit of the accelerator (compare with Fig. 4,b). The IB space charge overcompensation leads to an increase in the energy spread of the IB at the output of the cusp (see Fig. 5,c).

Fig. 6 show the computer simulation results for the acceleration of long compensated high-current IB (bunch length $36 \cdot z_I$) with additional IB space charge compensation by thermal electrons. The accelerating potential is 1 MB.

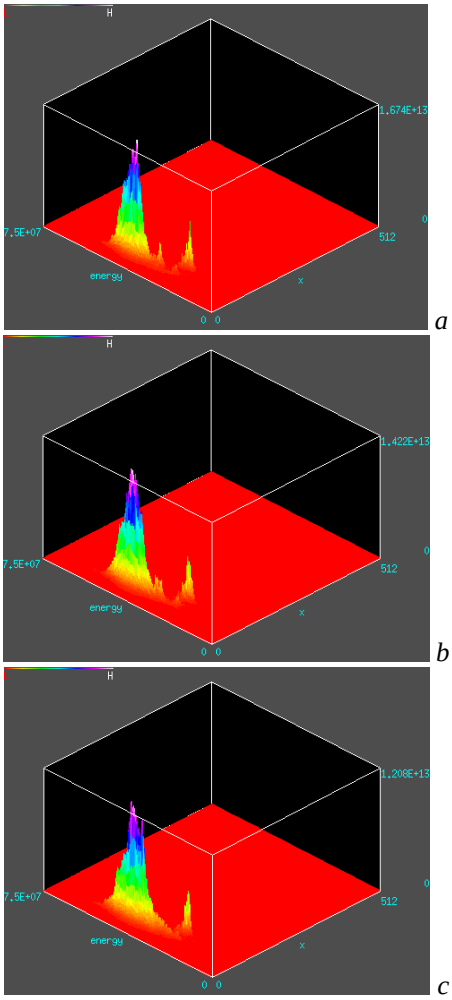

a *b* *c*

Fig. 5. IDFs vs energy and transverse coordinate at the exit of the cusp: a – at the time of the termination of the ME generation $n_e^{comp} = 0.5\, n_{i0}$; b – at the time of the termination of the ME generation $n_e^{comp} = 0.7\, n_{i0}$; c – at the time of the termination of the ME generation $n_e^{comp} = 1.0\, n_{i0}$. The ME generation occurs only in the right half of the cusp. The accelerating potential is 1 MB

The ME generation occurs in the left and right halves of the cusp, i.e., in the regions $[0, z_I] \times [r_{\min}, r_{\max}]$ and $[z_{II}, z_L] \times [r_{\min}, r_{\max}]$ (see Fig. 1). The ME generation starts at a time when the leading edge of the IB cross the left border of the appropriate drift gap, and stops when the leading edge of the bunch cross its right border. The generation rate is chosen so that at the time of its termination the ME electron density n_e^{comp} is $0.5\, n_{i0}$ (see Fig. 6,a), $0.7\, n_{i0}$ (see Fig. 6,b), and $1.0\, n_{i0}$ (see Fig. 6,c).

As can be seen from Fig. 6, an additional space charge compensation of the IB by ME in the left half of the cusp (before accelerating gap) leads to deterioration of the IDF, compared with the cases shown in Fig. 5.

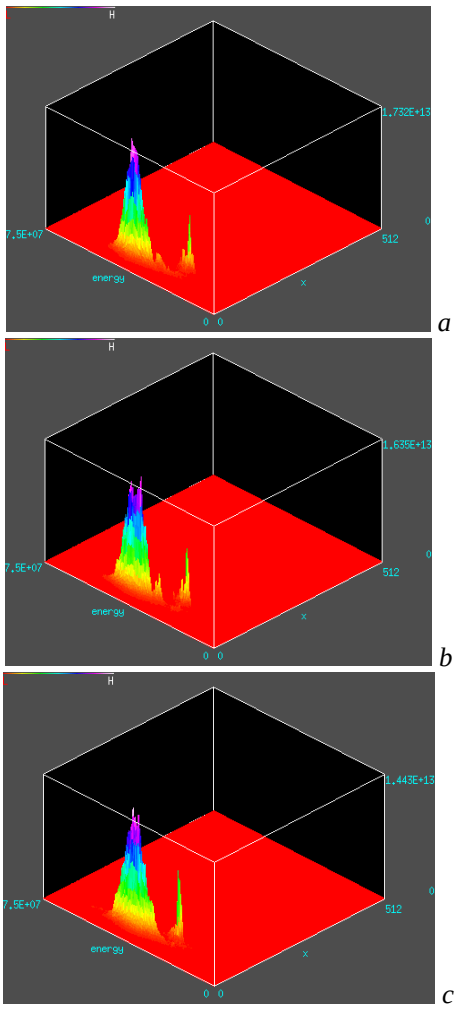

Fig. 6. IDFs vs energy and transverse coordinate at the exit of the cusp: a – at the time of the termination of the ME generation $n_e^{comp} = 0.5\, n_{i0}$ *; b – at the time of the termination of the ME generation* $n_e^{comp} = 0.7\, n_{i0}$ *; c – at the time of the termination of the ME generation* $n_e^{comp} = 1.0\, n_{i0}$ *. The ME generation occurs in the left and right halves of the cusp. The accelerating potential is 1 MB*

CONCLUSIONS

The particle in cell simulation results, within the limits of the complete set of the Maxwell-Vlasov equations, of the short (the ion bunch length is much smaller than the cusp length) and long (the ion bunch length is much longer than the cusp length) high-current compensated tubular ion bunches transportation and acceleration in the peaked fence magnetic field are presented. The ion bunch current, at injection in the cusp, is compensated by an accompanying electron bunch. Additional compensation of the ion bunch space charge by means of thermal electrons generated in the drift space has been studied. It is shown that both for short and for long ion bunches, the optimized in space and time additional space charge compensation by thermal electrons leads to a reduction of the energy spread of the accelerated ion bunch at the exit of the cusp.

REFERENCES

1. S.S. Yu, W.R. Meier, R.P. Abbott, et al. *An updated point design for heavy ion fusion:* Lawrence Livermore National Laboratory preprint. UCRL-JC-150169-REV-1, 2002, 10 p.
2. O.V. Batishchev, V.I. Golota, V.I.Karas', et al. Linear induction accelerator of charge-compensated ion beams for ICF // *Fizica Plazmy.* 1993, v. 19, №5, p. 611 (in Russian).
3. V.I. Karas', V.A. Kiyashko, E.A. Kornilov, Ya.B. Fainberg. Theoretical and experimental investigations of neutralized ion induction linac for ICF // *Nuclear Instruments and Methods in Phys. Res. A.* 1989, v. 278, №1, p. 245.
4. V.I. Karas', E.A. Kornilov, Ya.B. Fainberg. Linear induction accelerator of charge-compensated ion beams for ICF // *Problems of Atomic Science and Technology. Series "Plasma Electronics and New Methods of Acceleration" (1).* 1998, №1, p. 101.
5. V.I. Karas', V.V. Mukhin, V.E. Novikov, A.M. Naboka. About compensated ion beam acceleration in magnetoisolated systems // *Fizica Plazmy.* 1987, v. 13, № 4, p. 494 (in Russian).
6. N.G. Belova, V.I. Karas', Yu.S. Sigov. Numerical simulation of charged particle beam dynamics in axial symmetric magnrtic field // *Fizica Plazmy.* 1990, v. 16, №2, p. 209 (in Russian).
7. N.G. Belova, V.I. Karas'. Optimization of acceleration and charge neutralization of a high-current ion beam in two accelerating gaps of a linear induction accelerator // *Plasma Phys. Rep.* 1995, v. 21, №12, p. 1005.
8. V.I. Karas', N.G. Belova. Acceleration and stability of high-current ion beams in two accelerating gaps of a linear induction accelerator // *Plasma Phys. Rep.* 1997, v. 23, №4, p. 328.
9. O.V. Bogdan, V.I. Karas', E.A. Kornilov, O.V. Manuilenko. 2.5-d numerical simulation of high-current ion induction linac // *Problems of Atomic Science and Technology. Series "Nuclear Physics Investigations" (49).* 2008, №3, p. 34.
10. O.V. Bogdan, V.I. Karas', E.A. Kornilov, O.V. Manuilenko. 2.5-dimensional numerical simulation of a high-current ion linear induction accelerator // *Plasma Phys. Rep.* 2008, v. 34, №8, p. 667.
11. O.V. Bogdan, V.I. Karas', E.A. Kornilov, O.V. Manuilenko. Computer simulation of high-current ion induction linac using macroparticles // *Problems of Atomic Science and Technology. Series "Plasma Electronics and New Methods of Acceleration" (6).* 2008, №4, p. 83.
12. O.V. Bogdan, V.I. Karas', E.A. Kornilov, O.V. Manuilenko. High-current ion induction linac for heavy ion fusion: 2D3V numerical simulation // *Problems of Atomic Science and Technology. Series "Plasma Physics" (14).* 2008, №6, p. 110.
13. O.V. Bogdan, V.I. Karas', E.A. Kornilov, O.V. Manuilenko. Numerical simulation of a high-current ion linear induction accelerator with additional electron beam injection // *Problems of Atomic Science and Technology. Series "Nuclear Physics Investigations" (53).* 2010, №2, p. 106.

14. O.V. Manuilenko. Dynamics of the short high-current electron and ion bunches in the peaked fence magnetic field: 2d3v PIC simulation // *Problems of Atomic Science and Technology. Series "Nuclear Physics Investigations" (58).* 2012, №3, p. 183.
15. O.V. Manuilenko. Acceleration of the short high-current compensated ion bunches in the peaked fence magnetic field with additional space charge compensation by thermal electrons: 2D3V PIC simulation // *Problems of Atomic Science and Technology. Series «Plasma physics» (19).* 2013, №1, p. 146.
16. J.P. Verboncoeur, A.B. Langdon, N.T. Gladd. An object-oriented electromagnetic PIC code // *Computer Physics Communications.* 1995, v. 87, p. 199.

Article received 19.11.2013

ЧИСЛЕННОЕ МОДЕЛИРОВАНИЕ ТРАНСПОРТИРОВКИ И УСКОРЕНИЯ СИЛЬНОТОЧНЫХ ИОННЫХ СГУСТКОВ С ДОПОЛНИТЕЛЬНОЙ КОМПЕНСАЦИЕЙ ОБЪЕМНОГО ЗАРЯДА ТЕПЛОВЫМИ ЭЛЕКТРОНАМИ

О.В. Мануйленко, В.И. Карась

Приведены результаты численного моделирования методом макрочастиц в рамках полной системы уравнений Власова-Максвелла, транспортировки и ускорения коротких (длина ионного сгустка значительно меньше длины каспа) и длинных (длина ионного сгустка значительно больше длины каспа) сильноточных трубчатых ионных сгустков в магнитном поле остроугольной геометрии. Ток ионного сгустка при инжекции в касп скомпенсирован сопровождающим электронным сгустком. Изучена дополнительная компенсация объемного заряда ионного сгустка тепловыми электронами. Показано, что как в случае коротких, так и в случае длинных ионных сгустков оптимизированная дополнительная компенсация объемного заряда тепловыми электронами приводит к уменьшению энергетического разброса ускоряемого ионного пучка на выходе из каспа.

ЧИСЛОВЕ МОДЕЛЮВАННЯ ТРАНСПОРТУВАННЯ ТА ПРИСКОРЕННЯ ПОТУЖНОСТРУМОВИХ ІОННИХ ЗГУСТКІВ З ДОДАТКОВОЮ КОМПЕНСАЦІЄЮ ЇХ ОБ'ЄМНОГО ЗАРЯДУ ТЕПЛОВИМИ ЕЛЕКТРОНАМИ

О.В. Мануйленко, В.І. Карась

Наведено результати числового моделювання методом макрочасток у рамках повної системи рівнянь Власова-Максвелла, транспортування та прискорення коротких (довжина іонного згустка значно менше довжини каспа) та довгих (довжина іонного згустка значно більша за довжину каспа) сильнострумових трубчастих іонних згустків у магнітному полі гострокутової геометрії. Струм іонного згустка при інжекції в касп, скомпенсовано електронним згустком. Досліджено додаткову компенсацію об'ємного заряду іонного згустка за допомогою теплових електронів. Показано, що як у випадку коротких, так і у випадку довгих іонних згустків додаткова оптимізована компенсація об'ємного заряду тепловими електронами призводить до зменшення енергетичного розкиду іонного пучка, який прискорюється на виході з каспа.